Ultrasonics Sonochemistry 76 (2021) 105627

Contents lists available at ScienceDirect

Ultrasonics Sonochemistry

journal homepage: www.elsevier.com/locate/ultson

Study on the influence of advanced treatment processes on the surface properties of polylactic acid for a bio-based circular economy for plastics

Georgia Sourkouni [a], Charalampia Kalogirou [a,b], Philipp Moritz [a], Anna Gödde [a], Pavlos K. Pandis [b], Oliver Höfft [c], Stamatina Vouyiouka [b], Antonis A. Zorpas [d], Christos Argirusis [a,b,*]

[a] Clausthal Centre for Materials Technology (CZM), Clausthal University of Technology, Leibnizstr. 9, 38678 Clausthal-Zellerfeld, Germany
[b] School of Chemical Engineering, National Technical University of Athens, 9 Heroon Polytechneiou St., Zografou Campus, 15780 Athens, Greece
[c] Institute for Electrochemistry, Clausthal University of Technology, 38678 Clausthal-Zellerfeld, Germany
[d] Open University of Cyprus, Faculty of Pure and Applied Sciences, Environmental Conservation and Management, Laboratory of Chemical Engineering and Engineering Sustainability, P.O.Box 12794, 2252 Latsia, Nicosia, Cyprus

ARTICLE INFO

Keywords:
Micro-plastics
Pre-treatment of polymers
Sonochemistry
UV photochemistry
XPS
CLSM
AFM
DBD plasma
FTIR

ABSTRACT

New biotechnological processes using microorganisms and/or enzymes to convert carbonaceous resources, either biomass or depolymerized plastics into a broad range of different bioproducts are recognized for their high potential for reduced energy consumption and reduced GHG emissions. However, the hydrophobicity, high molecular weight, chemical and structural composition of most of them hinders their biodegradation. A solution to reduce the impact of non-biodegradable polymers spread in the environment would be to make them biodegradable. Different approaches are evaluated for enhancing their biodegradation. The aim of this work is to develop and optimize the ultrasonication (US) and UV photodegradation and their combination as well as dielectric barrier discharge (DBD) plasma as pre-treatment technologies, which change surface properties and enhance the biodegradation of plastic by surface oxidation and thus helping bacteria to dock on them. Polylactic acid (PLA) has been chosen as a model polymer to investigate its surface degradation by US, UV, and DBD plasma using surface characterization methods like X-ray Photoelectron Spectroscopy (XPS) and Confocal Laser Microscopy (CLSM), Atomic Force Microscopy (AFM) as well as FT-IR and drop contour analysis. Both US and UV affect the surface properties substantially by eliminating the oxygen content of the polymer but in a different way, while plasma oxidizes the surface.

1. Introduction

For several decades, environmental awareness has increased topics such as resource scarcity, climate change, waste production, costal erosion etc. which at the end have come into attention of several research activities which directly or intricately affect the civil society [1,2].

There are several strategies in place [1], which can be defined as a set of initiatives, which aim to minimize and control all kind of impacts, which arise from several processing and affect directly or indirectly the quality of life as well as the environmental performance of one area (even though a whole country). Among those strategies that aim to control and maintain any environmental issues and aspects are the circular economy, European Green Deal Strategy, United Nation Sustainable Development Goals and Bioeconomy [1,2,3,4,5]. Bioeconomy or Bio-circular economy or bio-based economy are applied taking into account existing political views and strategies, dedicated to support and strengthen the corresponding economy (i.e development of new jobs, technological achievements, optimization of environmental performance etc.) as well as, to deal with resource scarcity [6,7,8].

Polymer materials can be natural (cellulose, rubber etc.) but also synthetic from mineral oil stemming row materials. Since 1950 about 8300 million tonnes of plastics have been produced and have generated globally around 6300 million tonnes of plastic waste. Around 79% of this amount remains in the environment. It is estimated that, the continuation of current production and waste management trends will result in about 12 billion tonnes of plastic waste in natural environments by 2050 [9]. According to Laskar and Kumar [10] the last 10 years we

* Corresponding author.
E-mail address: amca@chemeng.ntua.gr (C. Argirusis).

https://doi.org/10.1016/j.ultsonch.2021.105627
Received 9 May 2021; Received in revised form 31 May 2021; Accepted 7 June 2021
Available online 10 June 2021

have produced and used more plastics, that we have used in the last 100 years. Hence, the amount of the plastics that entering the sea is near to 13 million tonnes per year. Based on that numbers, it is not surprising that plastics can be found almost everywhere in the environment, especially the marine environment, where large amounts of plastic waste accumulate with increased risks for humans and fauna [11]. Knowledge of the dangers and risks for people and the environment from chemicals in connection with the spread of plastic products in the environment is limited. WHO (World Health Organization) started to assess the potential risk of plastic pollution around the entire planet, to bring down the use of plastics [10]. Most of the raw chemicals used in the production of plastics stem from crude oil, and some are dangerous. These can be released during the manufacture as well as during the use and disposal of the plastic product [12].

Microplastics include fibers (mostly synthetic) and waste from plastics. Synthetic fibers are extremely harmful to any marine life [10] as the sea fish very often consume microplastics affecting in that way the food chain and the health directly, through the bloodstream. Anything less than 5 mm is being recognized as one of the largest threats to marine ecosystem. Major sources for microplastics in urban areas are agricultural greenhouses and single plastic bags. Even after the application of charges for plastic bags, in a recent work [13] have found up to seventeen different plastics in an urban wastewater treatment plant. Another microplastics source are soft drinks packaging materials [14], textiles as approximately two thirds of all those items are now synthetic, mainly organic polymers such as polyester, polyamide and acrylic, which can enter the environment either as primary particles with size in the range of mm or as microplastics after mechanical fragmentation and/or chemical or photochemical degradation [12,15]. A comprehensive review on the occurrence, accumulation and biological effects of microplastics in aquatic environments is given by Xu et al. [16].

According to Richard et al. [17] and Barnes et al. [18] the disposed of HD (High Density) as well as LD (Low Density) synthetic polymers (i.e. polyethylene, polyvinyl chloride, nylons etc.) is considered one of the very crucial environmental issues. Most of the microplastics in the sewage are removed by wastewater treatment plants, which remove microplastics by trapping them in the sludge and thus protecting aquatic environments from them. Nevertheless, there is evidence of strong microplastic accumulation in soils over time because of sludge applications on them [19].

Plastic microfibers (less than5mm) and nanofibers (less than100 nm) have been identified in ecosystems in all regions of the globe and have been estimated to comprise up to 35% of primary microplastics in marine environments, a major proportion of microplastics on coastal shorelines and to persist for decades in soils treated with sludge from wastewater treatment plants [20].

Recently a study of SU et al. [21] has shown, that more microplastics and polymer types are found in areas with large amounts of commercial, industrial and transport activities, near coastal cities but also in estuaries as microplastics are transported downstream in rivers. Increasing public concern is driving a vigorous research effort to create a complete circular economy for plastic waste. The development of bio-based depolymerization technologies and hence solutions to the world's plastic crisis is hampered by three main challenges: recalcitrant nature of plastics, non-biological degradability, and new technologies that must sustainably manage the constraints of highly plastic dependent lifestyles while addressing the global burgeoning plastic waste crisis in a low carbon footprint fashion. Several groups are now working on the problem of engineering enzymes with enhanced capacity to degrade plastic polymers such as polyethylene terephthalate (PET), a form of polyester [22].

Recent reviews are presenting the current status of polymer degradation based on microbial approach [23,24].

Microbes have a natural propensity to evolve in order to degrade new materials and thus to maintain nature's cycle of generation, degradation, and regeneration. However, several factors hindering the microbial and/or enzymatic degradation of plastics as well as other challenges can be associated to processes:

i. These processes are intrinsically slow and waste plastic substrates have only become prevalent in the past number of decades so that microbes did not have the time to adapt themselves to the degradation of the new materials;
ii. Despite the current extensive search for newly developed plastic-degrading bacteria and enzymes, only a limited number of strains were discovered that exhibit any activity in the degradation of plastics.
iii. The mechanisms behind the degradation of the plastic are very complex and thus concerted efforts are necessary to improve the efficiency of the used strains.
iv. There are several attempts to find new strains, whereat the focus was more on single strains and less on mixed consortia. For a broad mode of operation on the plastic degradation bacteria with diverse metabolic capabilities are needed. As an example, pseudomonas species with engineered properties to oxidize organic compounds can be named.
v. Another problem is that in presence of other easier to digest substances the bacteria attack them and not the plastics or the strains become inactive due to toxic additives for example due to non-intentionally added substances (NIAS) from the interaction of the plastic with other ingredients (e.g. food packaging) [25]. Therefore, the need to separate the plastics from other organic material is inevitable.
vi. The production of new enzymes that can be more active towards plastic degradation is difficult to scale-up for industrial use, meaning that at present plastics continue to accumulate in ecosystems [26].

It is known that polymers are degrading in the environment very slowly and that weathered plastics exhibit a rough surface and also chemical alteration of surface groups and bonds. Dong et al. [27] have characterized weathered and non-weathered polymers by means of Raman and FTIR spectroscopy and index them in a database. A similar approach based on Raman spectroscopy was used by Lv et al. [28] in order to detect microplastics and nanoplastics in aquatic environment. Besides the natural alteration one can use different techniques to degrade polymers such as biodegradation with enzymes and bacteria, thermal degradation, photolysis, chemical methods, high energy input methods like ultrasonication, microwaves etc. [29] and atmospheric DBD plasma [30]. Most of those processes (chemical degradation, as well as thermal [31] and enzymatic [32] methods) are working randomly and lead to unwanted mono- and oligomers and to modifications of the chemical microstructure of the side groups [33]. On the other hand, it has been reported by several authors, that ultrasonication represents a suitable method when products with lower molecular weight are desired [34,35].

UV represents a non-mechanical energy input method being able to degrade organic substances such as water-soluble pollutants but also solid organic waste such as plastics. Light can cause the decomposition of organic material and is one of the main causes of the degradation of plastic under ambient conditions. Most synthetic polymers can be degraded by the action of ultraviolet (UVA) radiation (400–290 nm) and visible light. UVA radiation possesses energies from 3.1 to 4.3 eV, which corresponds to 72–97 kcal/mol [36]. This means that it has enough energy to break most chemical bonds [37] and so light can act like thermal degradation [38].

Light absorption by chromophoric surface groups leads to the formation of radicals, which then interact with the polymer and lead to degradation [39]. Sonochemistry is a fast-developing branch of chemistry, which takes advantage of the ultrasound power. Sonochemistry is based on the effect of the acoustic cavitation, in which a sequential formation, growth and collapse of bubbles in a so-called hot spot leads to

harsh conditions that can strongly influence chemical reactions [40,41,42].

Ultrasound irradiation of a liquid causes the formation of cavitation bubbles in it. The bubbles can live several hundreds of μs and collapse upon reaching a critical radius! At this point, the collapsing bubble reaches locally (hot spot) extreme conditions with temperatures exceeding 5000 °C, pressures of more than 200 MPa and cooling rates of up to 10^{10} K/s [43]. In those cavitations, chemical reactions are easily running often through new pathways and mechanism [44,45,46]. Such conditions have been proven favorable to nanomaterial synthesis in terms of shorter reaction times, smaller particle sizes and phase-selectivity [47,48]. Additionally, cavitations can collapse on the surface of suspended solids and the generated solvent jets modify their surface itself (mechanically) and affect its properties (surface chemistry) [49]. Obviously, ultrasonication is a very effective method for energy input in chemical reactions, which easily can be upscaled to industrial scale [47]. Ultrasounds can break down the structure of the organic compound by either creating new non-toxic molecules or facilitating their oxidation by other processes. Additionally, they can be applied along with most advanced oxidation processes (AOPs), by contributing to additional production of •OH radicals, which benefit the oxidation process.

At the same time, UV assisted photochemistry can be also applied either stand-alone or in combination with ultrasounds in order to benefit from the improved potential due to the synergetic impact of the two methods.

It is well known that treatment of polymers with non-thermal plasma significantly affects their surface properties [50,51,52]. This can lead to a deterioration of the polymer surface, meaning that the surface starts already after a treatment of a few seconds to degrade [53]. On the other hand, the treatment of polymer surfaces by plasma leads to changes which can be beneficial for several applications. So, plasma treatment changes the surface energy, the adhesion on their surface, their wettability, concentration of surface chemical groups and thus to their catalytic activity to name only some of them [54].

Plasma treatment is mostly performed using cold plasmas at different atmospheres and pressures. If the treatment takes place in ambient atmosphere one speaks about treatment with atmospheric plasma. The simplest reactor design is the one with two parallel plates as electrodes and one or two ceramic dielectric barrier and kHz- powered sources [55,56,57,58].

The contribution of plasma generated atoms and radicals is significant. In air besides ozone, O atoms and OH radicals are generated and play an important role in several oxidation processes. Further, photons are generated, and thus plasma can act as a strong UV source for plastics and gaseous pollutants degradation as well as for water sterilization [56].

As it is known that bacteria and enzymes cannot digest plastics easily, the idea is to pre-treat the plastic surfaces using different advanced oxidation processes like ultrasounds, UV based photochemistry and their combinations as well as DBD plasma in order to increase the ability of the surfaces to let enzymes and bacteria dock on them and start the degradation process. The present work is the first step in the development of a holistic approach to degrade microplastics using biotechnological procedures. We start with pre-treatment steps using power ultrasound and UV-photochemistry and their combination in order to study synergistic effects on the accelerated degradation of the sample surface so that bacteria and enzymes can easier attack and degrade or even totally digest the microplastics. Additionally, to US and UV, we used also atmospheric plasma as a rapid surface treatment process (usually a few seconds or even less than one second), leading to an oxidation of the surface as oxygen plasma generates ozone within microseconds [59,60].

The presented results were obtained with polylactic acid (PLA), which was chosen as a model polymer easy to degrade. Careful experimental procedures and parameter variation during application of DBD plasma, high-power ultrasounds, and UV photochemical experiments, as well as application of surface sensitive characterization methods such as XPS, CLSM, AFM, IR, and drop contour analysis, are applied in order to elucidate degradation mechanisms and to further provide information for making the selection of bacteria and enzymes feasible, which in a subsequent biotechnological step can degrade and digest the microplastics.

2. Materials and methods

2.1. Materials

In this work a commercial polylactic acid (PLA) grade, Purapol L130 from Corbion was used for the film production by compression molding. Purapol L130 is a semi-crystalline, bio-based PLA grade, which is suitable for injection molding and fiber spinning. This PLA grade has high heat properties, medium flow and higher temperature resistance (viscosity average molecular weight M_v = 179000 g mol^{-1}, [COOH] = 7 meq kg^{-1}, $T_g = 70 \pm 1$ °C, $T_m = 180 \pm 1$ °C, melt flow index (ISO 1133-A at 210 °C/2.16 kg) = 16 g/10 min, Melt flow index (ISO 1133-A at 190 °C/2.16 kg) = 7 g/10 min). Purapol L130 has high optical purity, containing mainly L-isomer (min.99%). As it is recommended, Purapol L130 white pellets were dried in an oven at 100 °C, for 4 h prior to processing. PLA films (15x15cm) of approximately 1 mm thickness were prepared via compression molding. The material was brought up to the molding temperature (190 ± 2 °C) for 7 min, molded for 8 min under 200 ± 1 bar and then cooled down under compression to ambient temperature in ca. 10 min. The hot-pressed PLA foil was cut in samples with dimensions of 10x10 mm^2. These samples were used as reference for XPS and CLSM/AFM measurements and without further treatment directly in the ultrasound and UV-photochemical experiments. The treatment procedure is schematically presented in Fig. 1

2.2. Methods

2.2.1. Treatment methods of the PLA samples

2.2.1.1. Ultrasonication. Low-frequency Ultrasounds (20 kHz) were applied through the ultrasonic processor UIP500hdT (20 kHz, 500 W) from Hielscher Ultrasound Technology, Germany. Power intensity was fixed at 100 W/cm^2 through a 2.2 cm diameter tip. In several works [33,61,62,63] has been found that the degradation of different plastics is decreasing with increasing temperature mainly due to the cushioning effect, which reduces the intensity of the shock waves during the bubble collapse. On the other hand, increasing temperatures help the cleavage of chemical bonds on the surface. In any case, the degradation occurs at an optimum temperature [64]. In the present work, we performed at 20 kHz all experiments at constant temperature of 20 ± 1 °C.

High-frequency ultrasound was achieved by the Ultrasound Multi-frequency Generator equipped with the Ultrasound Transducer E805/T/M with 3 frequencies (approx. 0.550; 0.860; 1.150 MHz) and an adapted glass reactor UST 02/500–03/1500 from Meinhardt® Ultrasonics, Germany, with a maximum output power of 400 W/cm^2. The frequency was set to 860 kHz and the power amplitude to 40%. At 860 kHz it was necessary to keep the temperature constant at 30 ± 1 °C in order to protect the equipment, which may be damaged at temperatures above 50 °C. Temperature was controlled at 30 ± 1 °C using a Julabo recirculating cooler.

The PLA samples were suspended in demineralized water with a concentration of about 3 wt% without the addition of any other chemicals or additives and sonicated for 1 h under the conditions given above. After the sonication the samples were taken out of the suspension, dried in ambient air and kept dark until the XPS and CLSM/AFM measurements.

The treatment time for single sonication and UV experiments is 1 h

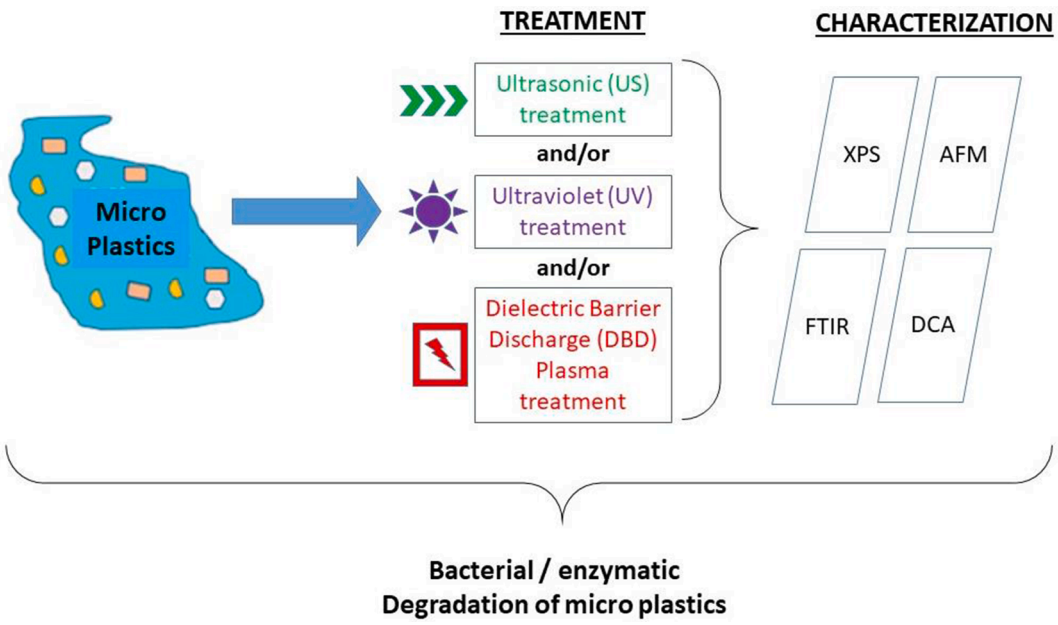

Fig. 1. Schematic presentation of the treatment and characterization procedure.

and for the combined experiments with US and UVA at the same time was 1 h. We performed also sequential treatment applying firstly US (at 20 kHz or 860 kHz) and afterwards UVA for a period of 1 h for each method leading to a total treatment time of 2 h. The last combination of US and UVA war performed by switching between US and UVA every 30 min for a duration of 1 h.

2.2.1.2. UVA treatment. The PLA samples were immersed in demineralized water in a UVA transparent baker and put on a stirring plate in the home-made UV reactor. The reactor has three 11 W UVA lamps on each side and thus the samples were exposed to 66 W UVA irradiation under continuous stirring. The treatment time was similar to the one we used for sonication. No photocatalytic active materials were used in the UV experiments. The samples were dried and kept dark after finishing of the UVA irradiation experiment.

2.2.1.3. DBD plasma treatment. The PLA samples with dimensions of 30x30 mm^2 and 390 μm thickness were used as received and put in a self-made parallel plate dielectric barrier discharge (DBD) reactor with their marked surface up in order to treat them with an atmospheric DBD plasma at ambient air. The DBD plasma conditions were 16 KV at a frequency of 7 kHz and the distance between the electrodes was set to 3 ± 0,1 mm. The samples were treated for 5, 10, 20 and 60 s and then the samples were immediately transferred to the FTIR, CLSM/AFM, and XPS devices in order to characterize the changes on the surface groups caused by the plasma treatment.

After the FTIR measurements the wettability of the same sample was immediately measured in a drop contour analysis device.

2.3. Characterization methods of the PLA samples

2.3.1. X-Ray photoelectron spectroscopy (XPS)

XPS a surface sensitive characterization method that uses by single-energy X-ray photons with kinetic energies from 300 to 1500 eV to irradiate the sample surface and detects photoelectrons emitted from the samplés surface. XPS or electron spectroscopy for chemical analysis (ESCA) is a relatively simple technique that allows for the compositional and chemical state analysis of surfaces. Using XPS one can estimate the composition of a surface by quantitative elemental analysis as all elements, with the exception of hydrogen and helium, can be detected through the detection of the binding energies of the photoelectrons. Because of the short path length of the used photoelectrons XPS is very surface sensitive [65,66].

For XPS measurements, the US and UV-treated PLA samples were fixed with a stainless-steel sample holder and inserted into the XPS apparatus. The PLA samples were analyzed by XPS in an ultrahigh vacuum (UHV) chamber, with a base pressure below $5{\cdot}10^{-10}$ mbar. The detailed apparatus setup was described previously [67,68]. A commercial X-ray source (RS40B1, Prevac, Rogów, Poland) was used to generate non-monochromatic MgKα X-rays, which hit the surface under an angle of 10°. The electrons emitting from the PLA samples were analyzed by a hemispheric analyzer (type Leybold EA10/100) under an angle of 45°. The analyzer was operated with a constant pass energy of 80 eV for survey spectra and 40 eV for detail spectra. In order to keep radiation damage to the PLA as low as possible, detail spectra were first recorded, followed by the corresponding survey spectrum. All XP spectra are displayed as a function of binding energy with respect to the Fermi level. Since the PLA samples have a low electrical conductivity, the XP spectra had to be charge-corrected. The aliphatic C–C binding at 285.0 eV was used as a reference. For a stoichiometric evaluation, a linear background correction was applied. A detailed analysis of the photoelectron peaks was performed using Voigt-type profiles and Tougard base line type with CasaXPS software (version 2.3.16 Pre-rel 1.4, CasaXPS Ltd., Teignmouth, United Kingdom).

2.3.2. Confocal laser Scanning Microscopy (CLSM) and atomic Force Microscopy (AFM)

Confocal Laser Scanning Microscopy (or CLSM) is an optical imaging technique widely used in the field of Materials Science. CLSM provides high optical resolution and observation precision by combining the colour and laser intensity information from the camera and from the laser light photoreceptor, respectively.

We used a Keyence VK-X100K/X-200 K Confocal Laser Scanning Microscopy (CLSM) in which a sample is illuminated by laser source, and the scattering or fluorescence intensity of a certain volume element are measured. In CLSM the size of the scanning volume is determined by the used spot size. The average roughness (R_a) represents the mean value of the roughness profile determined from deviations about a line within the surface and R_q the root-mean-square roughness. All R_a and R_q values are mean values of at least two measurements. In addition to surface

roughness measurements (R_a, R_q), CLSM provides surface profile observation in 3-D images, by capturing multiple two-dimensional images at various depths, to confirm the shape and scrutinize how each pre-treatment method affects the surface of PLA samples.

CLSM is the first choice in our surface microscopy methods as it allows a quick estimation of surface roughness, while AFM is mostly used to control the CLSM results and to estimate mechanical properties of the treated plastic samples. By using the AFM as nano-intender one is also able to measure the mechanical properties of a sample with a nanometric resolution [69,70,71,72].

2.3.3. Attenuated total reflection fourier transform infrared spectroscopy (ATR-FTIR)

Infrared spectroscopy is based on the principle of absorption of electromagnetic radiation of the infrared spectrum by molecules, resulting in molecular vibrations.

The absorption energies can therefore be associated with certain vibrational modes of the chemical bonds. Each molecule has a specific absorption depending on the atomic bonds. This makes it to a common analysis technique for obtaining chemical information of the surface of a material.

The infrared analysis of the PLA samples is performed on a Bruker Alpha-T FTIR Spectrometer. It is coupled with an Attenuated Total Reflection (ATR) accessory. The internal reflection element is a diamond crystal and by pressing the sample onto the ATR crystal, the ATR enables a simple procedure to obtain IR spectra.

2.3.4. Drop contour analysis (DCA)

In drop contour analysis, a treated sample and a water drop on top of it are video recorded against a backlight. The contact angle can then be determined by the software. The estimated contact angle is the most important value in order to characterize the wettability of a surface. The higher the surface tension between the solid and the atmosphere, the higher is the surface energy of the solid. The drop will attempt to spread out, which results in a small contact angle. In this study we used a Dataphysics OCA device allowing the video analysis of the drop contour.

3. Results

The experiments presented are single treatment experiment with only US at 20 kHz or at 860 kHz and UVA but also experiments with simultaneous use of UVA plus US at both frequencies (one frequency in each experiment). In order to verify if the order of application of each treatment method plays a role in the final result, we performed experiments with US and UV in a sequential way and also alternating between US and UVA every 30 min.

3.1. XPS and CLSM/AFM results

The samples have been treated for 1 h using ultrasounds at frequencies of 20 kHz and 860 kHz as well as UV light with wavelength between 400 and 315 nm with a maximum at 365 nm (UVA). After the UV exposure experiments the samples have been analysed by means of XPS and CLSM/AFM.

In Fig. 2 the XPS spectra of the pre-treated samples are presented. The XP survey spectrum (not shown here) contains the main photoelectron peaks of carbon (C1s) and oxygen (O1s). The C1s and O1s detail spectra (derived from the survey spectrum) show the binding species (C–C/C–H, C-O, O = C-O) typical for PLA, whose binding energies correspond well with the literature [73,74]. The excessive proportion of C–C bonds is due to atmospheric contamination.

As a result of the treatment procedures described in section 2 one can expect a change in the surface elemental composition and in the particular case of plastic materials a change in the C/H and C/O ratio as compared to the untreated surface. The changes in the total C/O stoichiometry resulting from the XPS analysis are summarized in Table 1. As

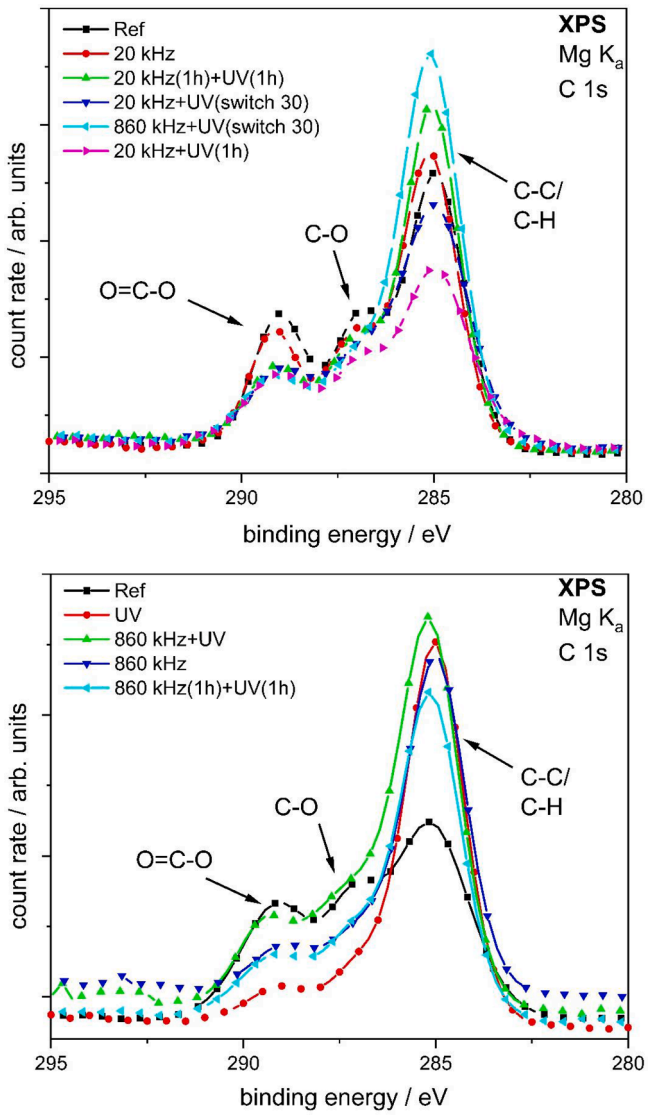

Fig. 2. XPS spectra of the surface indicating the composition of the PLA samples treated with different methods for 1 h.

can be seen in Table 1 and the detail spectra (Fig. 2) the surface composition changes significantly as C-O and O = C-O groups on the surface are diminished depending on the method (UV or US) and US frequency used. The same species as in the PLA reference were used for peak deconvolution (not shown). However, it has to be mentioned, that it cannot be ruled out that further C-O_x species were formed during the treatments in the water.

The CLSM measurements tabulated in Table 2 show a smooth surface with slightly increased root mean squared roughness as compared to the reference sample. Treatment with US at 20 kHz seem to lead to a slightly lower surface roughness.

By comparing the results of the combined experiments of simultaneous application of US and UV (Table 1) it is evident that there are no synergetic effects from the simultaneous use of US and UV as the values are lower than the value for sole use of UV. Especially the use of UV and high frequency US at 860 kHz is counterproductive as the resulting value is lower than UV and also US at 860 kHz alone. This is surprising, as it seems that the two treatment methods inhibit each other.

The XPS results (spectra not shown) of the plasma treated samples are summarized in Table 3. In this study we used a second batch of PLA samples as the first batch was used for all other techniques. This explains the slight difference in the surface composition of the reference sample.

Table 1
Surface composition of PLA depending on the pre-treatment method. Treatment time for all experiments in this table was 1 h except for the sequential experiments where the time was 1 h for each sequence.

Sample name	survey spectrum			C1s			O1s	
	C1s [at%]	O1s [at%]	N1s [at%]	C -C [at%]	C - O [at%]	C = O [at%]	C - O [at%]	C = O [at%]
Reference	63,92	36,08	0	53,59	22,31	24,09	47,20	52,80
UVA	80,12	19,88	0	82,06	11,08	6,86	70,58	29,42
20 kHz	64,98	35,02	0	59,00	20,88	20,12	48,19	51,81
(20 kHz + UV) (1 h)	64,70	34,25	1,06	59,02	17,64	23,34	83,42	16,58
20 kHz(1 h) + UV(1 h)	66,84	31,16	2,01	65,36	18,79	15,86	54,86	45,14
20 kHz + UV(switch30)	69,44	29,37	1,2	63,80	18,95	17,25	49,69	50,31
860 kHz	70,24	29,76	0	76,58	14,96	8,47	85,47	14,53
(860 kHz + UV) 1 h	65,25	33,56	1,2	60,92	28,88	10,20	69,09	30,91
860 kHz(1 h) + UV(1 h)	71,96	26,40	1,64	69,84	15,49	14,67	45,65	54,35
860 KHz + UV(switch30)	75,39	24,61	0	72,98	13,27	13,75	60,81	39,19

Table 2
Change of the PLA surface roughness parameters depending on the used pre-treatment method.

Roughness	Reference	UV	20 kHz	860 kHz	20 kHz + UV	860 kHz + UV	20kHz + UV switch	860 kHz + UV switch	20 kHz + UV seq	860 kHz + UV seq
R_a	9,10	9,29	8,36	11,05	7,80	14,88	9,38	11,95	10,50	13,75
R_q	11,74	11,69	11,06	13,38	10,25	18,53	11,88	15,43	13,03	17,11

Table 3
Elemental composition of the PLA surface after plasma treatment derived from the XPS spectra.

Sample name	Survey spectrum		C1s			O1s	
	C1s [at%]	O1s [at%]	C - C [at%]	C - O [at%]	C = O [at%]	C - O [at%]	C = O [at%]
Reference	59,44	40,56	40,36	33,33	26,30	33,08	66,92
PLA-Plasma-5 s	61,54	38,46	48,31	27,77	23,92	46,11	53,89
PLA-Plasma-10 s	53,71	46,29	39,23	34,99	25,78	43,05	56,95
PLA-Plasma-20 s	55,93	44,07	34,05	34,93	31,02	45,08	54,92
PLA-Plasma-60 s	60,24	39,76	35,06	32,76	32,18	44,62	55,38

The surface is clearly oxidized by the plasma treatment. Already after 10 s of treatment the surface is 10% more oxidized. By deconvolution of the C1s peak (not shown or supplement) in the possible binding types we obtain the percentage of single and double bonded oxygen atoms to carbon.

The surface changes caused by the plasma treatment are also detectable by roughness measurements using CLSM (Table 4).

3.2. FT-IR results

Each sample was analyzed by means of FT-IR to document changes in the concentration of chemical groups on their surface caused by the treatment.

In Fig. 3 we present FT-IR spectra of all treated samples for 1 h.

Obviously, the concentration of the active surface groups is changing depending on the treatment method. The difference in peak intensities suggests a concentration change of functional groups.

In IR spectra at 1747 cm^{-1} the C = O stretching region appeared as a broad asymmetric band mainly due to active modes. The peak at 1455 cm^{-1} appear because of the band CH_3. The CH deformation and asymmetric bands appeared at 1378 cm^{-1} and 1359 cm^{-1} and the CH bending modes resulted in bands at 1315 cm − 1 and 1300 cm^{-1}. At 1267 cm^{-1} appeared the C–O stretching modes of the ester group and at 1085 cm^{-1} the C–O–C asymmetric mode. The peak at 953 cm^{-1} is due to bands characteristic of helical backbone vibrations with CH_3 rocking. At 862 cm^{-1} the band could be attributed to the amorphous phase of PLA or to C–C stretching. At 747 cm^{-1} appeared the band that could be attributed to the crystalline phase of PLA, or even to C = O stretching.

Further we investigated the surface groups changes as a function of the plasma treatment time. The results presented in Fig. 4 are mean values from spectra at three different places on the surface. There is a strong influence of the plasma treatment on the concentration of the surface groups (especially oxygen containing groups like C = O and C-O-C, which content increased by ca. 8%) and a non-linear dependence of them on the plasma treatment time. The highest concentration is observed after 10 s of plasma treatment.

Table 4
Surface roughness parameter of the plasma treated samples immediately after the treatment procedure.

	Reference	5 sec	10 sec	20 sec	60 sec
R_a	3.32	2.05	2.61	2.09	6.06
R_q	4.16	2.75	3.31	2.74	7.29

3.3. Drop contour analysis results

The results of the drop contour analysis are an indicator of the hydrophilicity or hydrophobicity of the polymer surface. The values presented in Fig. 5 are the values of the two angles the left- and right-hand side of the drop. The mean deviation in all measurements is less than 2°.

Obviously, all treatment methods and their combinations increase the hydrophobicity of the PLA surface.

Among the used single treatment methods US at 860 kHz and UVA seem to have the highest impact on the wettability of the surface. In the combined treatment with ultrasounds and UVA the UVA impact is persisting and the combination of US at 860 kHz with UVA exhibits the highest contact angle of 101.5°.

In Fig. 6 we present DCA results of plasma treated PLA samples. In this case the influence if the treatment is positive, as the hydrophobicity is decreased. It has been reported [75,76] that the surface of plastics after plasma treatment does not remain in the new state for long time. We performed an additional measurement of the contact angle after 6 days to find out if this is the case in our plasma treated samples.

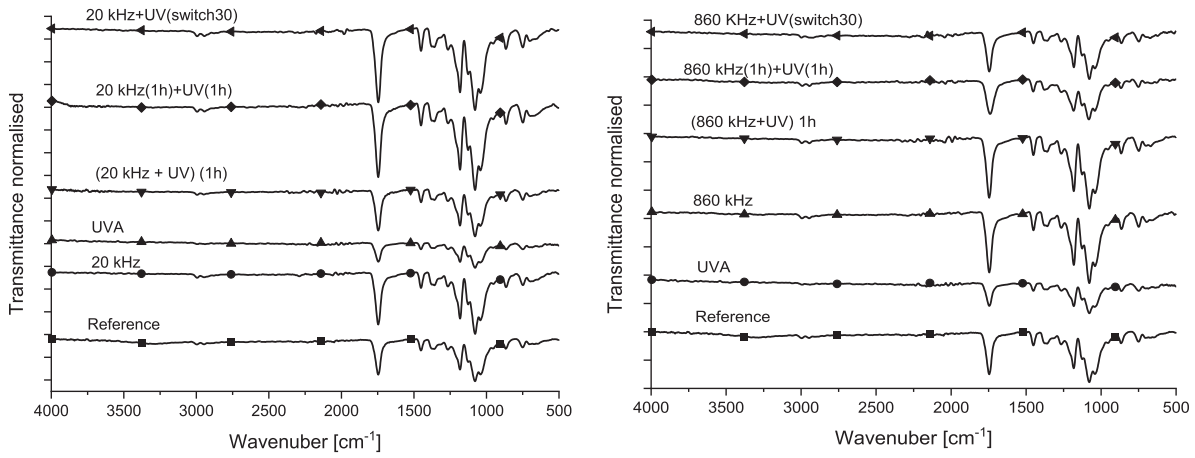

Fig. 3. FT-IR spectra of samples treated for 1 h by different methods. US at 20 kHz and its combinations with UVA (left) and US at 860 kHz and its combinations with UVA (right).

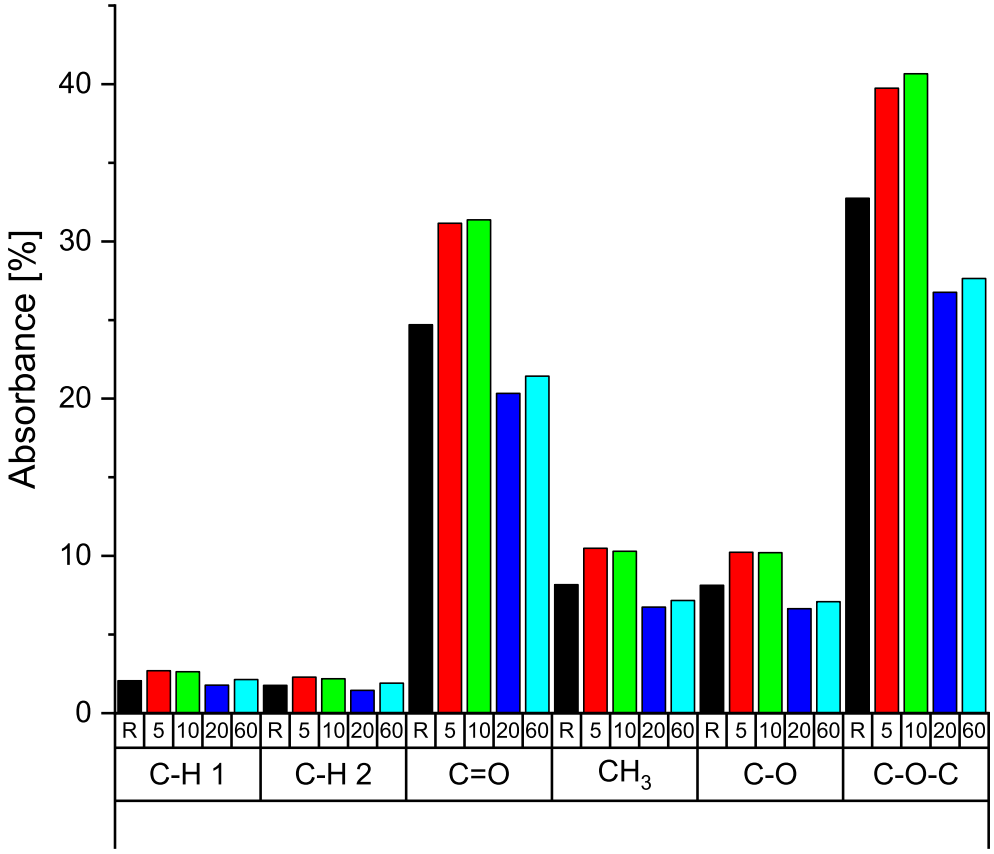

Fig. 4. Absorbance of surface groups derived from FT-IR spectra. The upper X-axis indicates the treatment time, where R is the reference material. The lower X-axis indicates the vibrational group on the surface.

4. Discussion

Looking closer on the XPS results in Table 1 it seems that based on the survey spectrum, sonication at 20 kHz does not substantially change the surface composition as compared to the reference sample but there are rearrangements between carbon and oxygen. Obviously, C–C bonds are increasing by ca. 5% due to the fact that both C-O and C = O concentrations decrease. The PLA surface is less oxidized as compared to the one of the reference sample. This shows that the US energy input is either not sufficient to largely rearrange the surface or the US produced radicals are not reactive enough in order to further oxidize the PLA surface. The results show a weak interaction of the 20 kHz US with the PLA surface and correlate with the roughness mean value of its surface which remains close to the one of the reference sample Table 2.

At 860 kHz the US-initiated cavitation seems to be more active and thus the interaction not only diminishes the oxygen containing groups but also strongly affects the roughness of the sample surface and increases the R_a factor from 9.1 to 11.05.

The high ultrasound frequency seems to affect more the surface of the sample, while the low frequency of 20 kHz seems to induce only a slight change as compared to the non-treated sample. This implies that the cavitation energy and its impact at 860 kHz is more active regarding

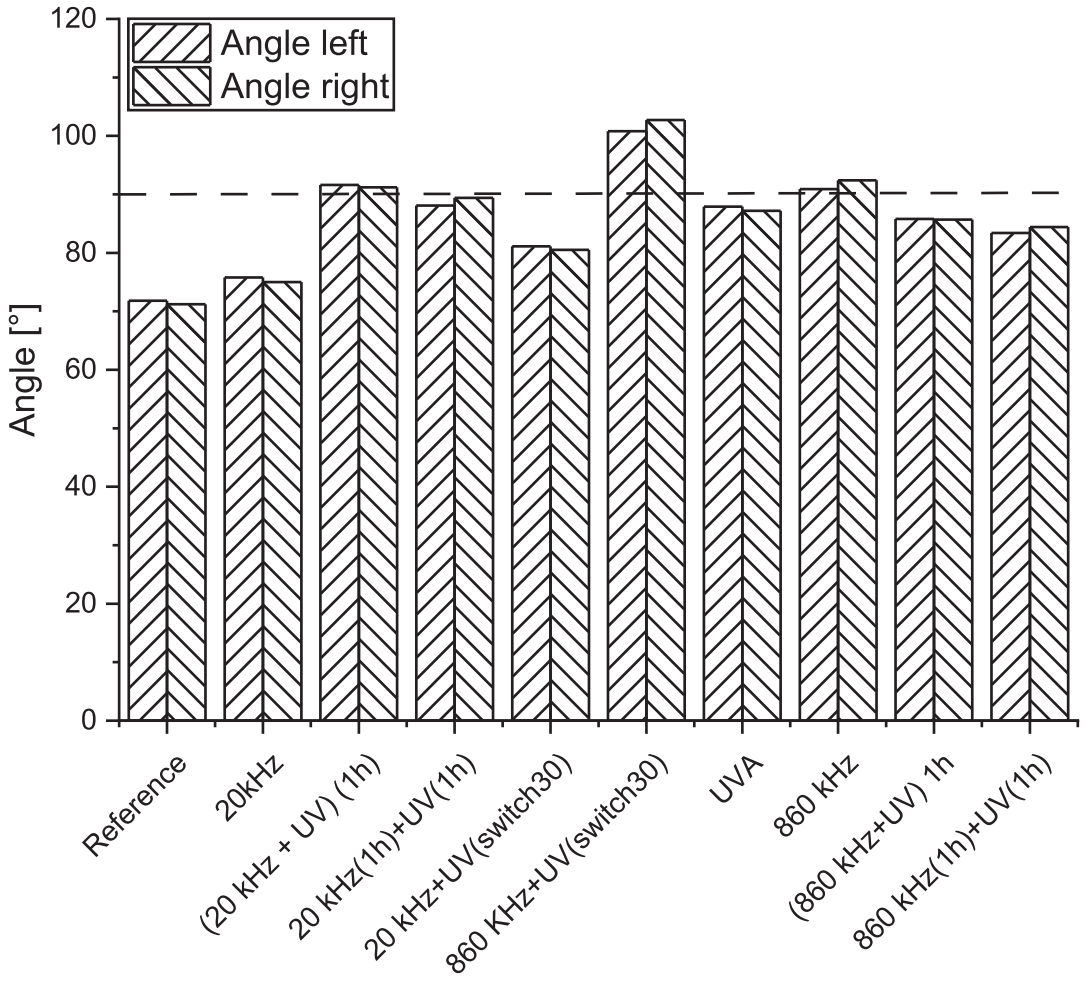

Fig. 5. Contact angle resulting from the drop contour analysis (on both sides) of the samples treated for 1 h using US, UVA and their combinations. The line at 90° indicates the angle above which the surface is considered more hydrophobic.

surface modification of the PLA samples. This may be related to the fact that at 860 kHz we have a larger number of tiny microbubbles for the same period of time as compared to 20 kHz that, instead of imploding vigorously (due to small size, surface tension etc.) as in 20 kHz, have a vigorous oscillating behaviour scrubbing and altering the surface of the sample possibly similar to the exfoliation mechanism of graphite to graphene [77].

From the UV experiment can be concluded that UV irradiation is more active than ultrasonication regarding cleavage of the C-O and O = C-O bonds but does not affect the surface roughness as it does not act mechanically. The chemical attack induced by UV irradiation is more important regarding the chemical surface modification as compared to the more mechanical impact of the ultrasound. The surface composition changes are highest in the UV experiment.

All the above findings are confirmed by the FT-IR findings. In the spectra in Fig. 3 the C = O stretching region appearing at about 1747 cm^{-1} as a broad asymmetric band follows and confirms the XPS findings tabulated in Table 1.

The experiments with combined treatment methods do not exhibit an increased de-oxidation of the surface as expected from a synergy of the two applied methods.

Considering the experiments with 20 kHz US and UVA simultaneously for 1 h we observe practically the same C1s concentration (64.98%) as in the pure 20 kHz US experiment (64.70%). The only change is observed in the C = O concentration which is decreased with UV. In the experiment with sequential application of 20 kHz US followed by UVA the influence by UVA is increased and C1s reaches 66.84%. This behavior becomes stronger when we perform the experiment by switching between US and UVA every 30 min (first US followed by UVA).

Similar tendency is observed using US at 860 kHz despite a slightly stronger effect due to the high US frequency.

Interestingly, despite the increasing C–C bonds concentration using both kinds of US and UVA none of the experiments reaches the C–C bonds concentration reached by UVA alone (80.12%).

The question arising from this observation, is why the combination of US and UV irradiation does not lead to higher decomposition of the surface? One would expect oxygen contents of less than 19.88%, which is the lowest value observed in the two methods acting alone (using UVA). In fact, we observe a negative synergy of US and UVA. One explanation for this observation could be the mechanical removal of parts of the surface bringing continuously fresh PLA to the surface leading to an erroneously increased oxygen groups content. Another explanation could have to do with the hindrance of the UV irradiation to reach the samples due to the strong cavitation, i.e. the UV light is reflected on the bubble clouds and thus less UV irradiation reaches the surface of the PLA samples.

A totally different picture is evident, when DBD plasma is used as surface treatment method. In this case after a short period of up to 5 s, which most probably is necessary for the plasma to become stable, we observe an oxidation of the surface at a treatment time up to 20 s.

The reason for the increased values at time up to 20 s Fig. 4 and not any more at 60 s is that plasma etching often takes place as a competitive reaction to plasma-induced functionalization. This leads to a partial

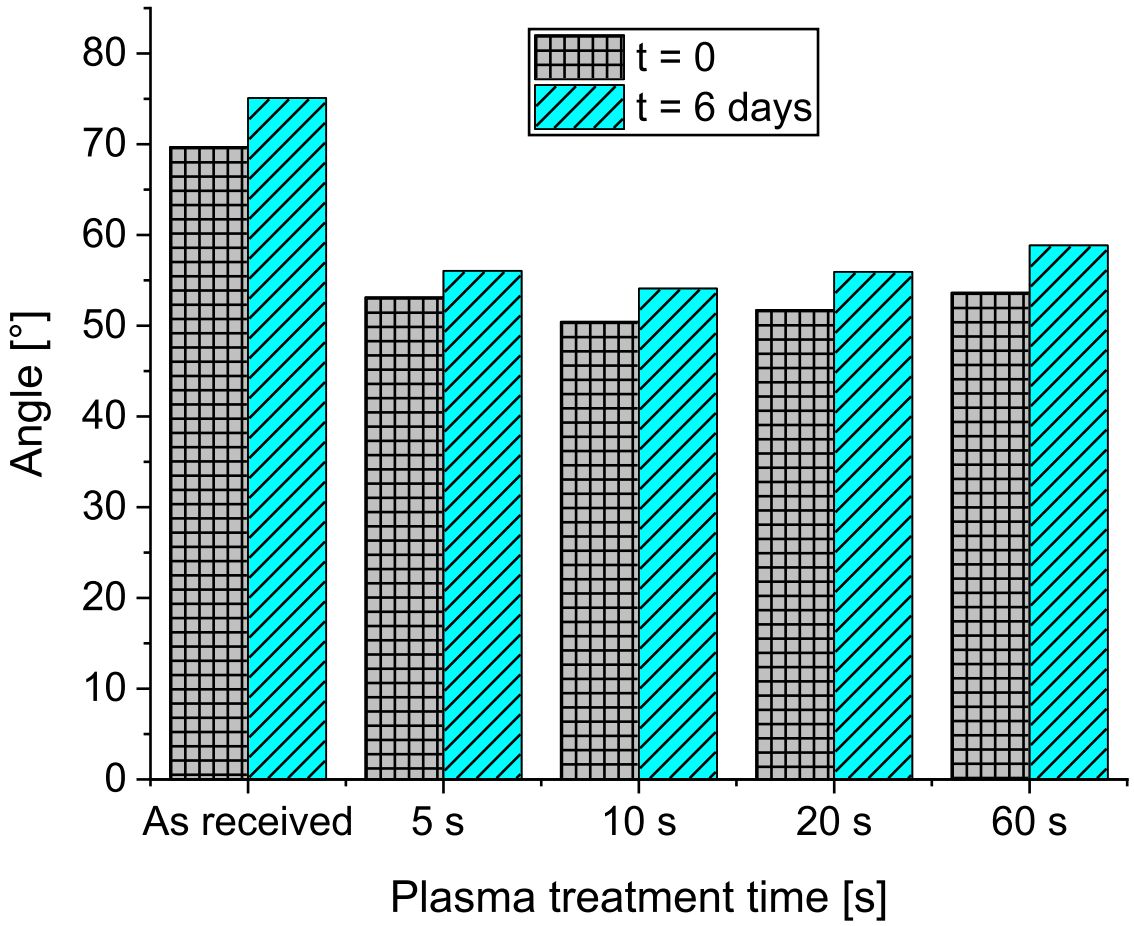

Fig. 6. Contact angle resulting from the drop contour analysis of samples treated using DBD plasma. The samples have been measured once again after six days to find out if the surface properties are changing with time.

degradation of already functionalized surface areas, with longer treatment times leading to a steady equilibrium between the plasma-induced functionalization and the plasma-induced degradation of the surface [78].

The changes on polymer surfaces caused by an oxygen plasma can be sometimes, according to some publications, not resistant to aging, an effect which manifests itself in a reduced wettability with increasing storage time [77]. The decreasing wettability of the polymer surfaces can be attributed to various effects. On the one hand, a thermodynamically controlled reorientation is responsible for this, in which the polar groups rotate away from the surface into the area close to the surface [79]. On the other hand, this phenomenon can be explained by a migration of oxidized oligomer fragments from the surface into the bulk area, which is due to an increased mobility of the polymer chains in the polymer surface compared to the bulk area. Morra et al. [80] reported on the aging behavior of PP films treated in O_2 plasma as a function of temperature. It was found that the wettability of the stored PP films decreased more rapidly with increasing temperature. The reason for this behavior is an increased diffusion rate at higher temperatures.

Nevertheless, we did not observe a deterioration of the plasma induced surface properties after 6 days. We believe that the aging effect depends on the stability of the surface groups induced by the plasma treatment and this has directly to do with the properties of the used plasma. We kept the samples at room temperature but in dark conditions, so that the temperature effect of the diffusion discussed by Morra et al. [80] does not hold.

Finally, the results of the drop contour analysis confirm the abovementioned behavior as US and UVA as well as their different combinations lead to a more hydrophobic PLA surface in accordance with the decreased surface oxygen content. On the other hand, DBD plasma oxidizes the surface according to the XPS and FT-IR findings and this is apparent in the DCA results where all DBD plasma treated PLA samples exhibit a higher hydrophilicity.

A complete degradation of PLA in soil and water may take up to several years [81,82] mainly because PLA is resistant to environmental bacteria. The degradation process is initialized by chemical hydrolysis [83] of polymeric PLA into oligomers that are then transformed into carbon dioxide and water by environmental microorganisms producing specific enzymes. We suggest that plasma pre-treatments of PLA developed here may accelerate degradation process through both decreasing the molecular weight of PLA and optimizing bacterial efficiency. Only few PLA-degrading soil microorganisms were identified [84], and all decompose PLA under aerobic conditions [85]. This suggests that oxygen availability on the plasma-treated PLA surface would significantly enhance biodegradation process in the soil.

5. Conclusions

Three different advanced oxidation methods (ultrasounds at 20 and 860 kHz, UVA irradiation, and DBD plasma) as well as combinations of US and UVA have been used to degrade PLA as a model polymer for micro-plastics.

Ultrasonication affects the surface chemistry as well as the morphology by increasing the roughness of the sample. Especially when the high frequency of 860 kHz is used R_a is increased from 9.1 to 11.05 and to 14.88 when US at 860 kHz is used together with UV irradiation. The C/O ratio of 1,77 in the pristine sample is increased in both sonication methods with higher impact at 860 kHz (1.85 at 20 kHz and 2.36

at 860 kHz). The highest impact on the C/O ratio is observed when using IV irradiation (C/O ration of 4,03) concluding that UV photodegradation is more active than the two-ultrasonication methods for the de-oxidation of the PLA surface.

A combination of both US and UV pre-treatment methods does not lead to the expected synergetic effects and the change in the C/O ratio is less as compared to the UV pre-treatment alone. The reason for that could be either a suppression of the UV intensity due to the formation of cavitation bubbles or the ultrasonic abrasion of the surface layer bringing fresh PLA to the free surface and thus changing the C/O ratio to lower values.

This is not beneficial for a possible subsequent enzymatic or bacterial degradation of the PLA as bacteria are more active on oxygen reach surfaces.

The treatment of the PLA surface using DBD plasma leads to the desired increased oxygen content of the PLA surface by 5,73% after 10 s treatment.

The degradability of the differently pre-treated samples has to be experimentally investigated in future biotechnological studied using different bacterial strains.

Declaration of Competing Interest

The authors declare that they have no known competing financial interests or personal relationships that could have appeared to influence the work reported in this paper.

Acknowledgements

We are indebted to Dr. Jasmina Vidic (INRAE, Université Paris-Saclay, Paris, France) and Dr. Jasmina Nicodinovic-Runic (IMMG, University of Belgrade, Serbia) for valuable discussions on the docking mechanisms of bacteria on polymer surfaces.

Author's contributions

GS, CA, and AZ searched the literature and obtained all references used in this manuscript. CA, GS, and AZ wrote the manuscript draft, read, corrected, and approved the final manuscript.

CA contributed to the study conception and design. Material preparation, data collection and analysis were performed by GS, CK, MV, PP, AG, PM and OH. Quality control of the data and analyses were performed by CA and GS. GS and CA supervised the findings of this work and all authors contributed to the interpretation of the results. All authors read and approved the final manuscript.

Funding

The authors declare that this study has been partly funded from the European Unioń s Horizon 2020 research and innovation programme under grant agreement number 870292 (BioICEP).

Data Availability

Most of the data generated or analysed during this study are included in this published article and in the supporting information file. Some FT-IR and XPS spectra and related information data are available on request from the authors.

Compliance with ethical standards

Ethical approval Not applicable.

Consent to participate

All authors consented to participate in this manuscript.

Consent for publication

All authors consented to publish the results of this study.

References:

[1] S. Bröring, N. Laibach, M. Wustmans, Innovation Types in the bioeconomy, J. Cleaner Prod. 266 (2020) 121939, https://doi.org/10.1016/j.jclepro.2020.121939.
[2] Loizia, P., Neofytou, N., Zorpas, A.A. 2018 The concept of circular economy in food waste management for the optimization of energy production through UASB reactor Environmental Science and Pollution research, https://doi.org/10.1007/s11356-018-3519-4.
[3] D. Symeonides, P. Loizia, A.A. Zorpas, Tires Waste Management System in Cyprus in the Framework of Circular Economy Strategy» Journal of, Environ. Sci. Pollut. Res. (2019), https://doi.org/10.1007/s11356-019-05131-z.
[4] Y.V. Fan, J.J. Klemeš, T.G. Walmsley, B. Bertók, Implementing Circular Economy in municipal solid waste treatment system using P-graph, Sci Total Environ. 701 (2020) 134652, https://doi.org/10.1016/j.scitotenv.2019.134652.
[5] M. O'Brien, D. Wechsler, S. Bringezu, R. Schaldach, Toward a systemic monitoring of the European bioeconomy: gaps, needs and the integration of sustainability indicators and targets for global land use, Land Use Pol. 66 (2017) 162–171, https://doi.org/10.1016/j.landusepol.2017.04.047.
[6] C. Priefer, J. Jörissen, O. Frör, Pathways to shape the bioeconomy, Resources 6 (1) (2017) 10, https://doi.org/10.3390/resources6010010.
[7] N. Antoniou, A.A. Zorpas, Quality Protocol Development to define End-of-Waste Criteria for Tire Pyrolysis Oil in the framework of Circularl Economy Strategy, Waste Manage. 95 (2019) 161–170, https://doi.org/10.1016/j.wasman.2019.05.035.
[8] R. Geyer, J.R. Jambeck, K.L. Law, Production, use, and fate of all plastics ever made, Sci. Adv. 3 (7) (2017) e1700782, https://doi.org/10.1126/sciadv.1700782.
[9] N. Laskar, U. Kumar, Plastics and microplastics: A threat to environment, Environ. Technol. Innovation 14 (2019) 100352, https://doi.org/10.1016/j.eti.2019.100352.
[10] R. Hurley, J. Woodward, J. Rothwell, Microplastic contamination of river beds significantly reduced by catchment-wide flooding, Nat. Geosci. 11 (2018) (2018) 251–257, https://doi.org/10.1038/s41561-018-0080-1.
[11] D. Lithner, Å. Larsson, G. Dave, Environmental and health hazard ranking and assessment of plastic polymers based on chemical composition, Sci. Total Environ. 409 (18) (2011) 3309–3324, https://doi.org/10.1016/j.scitotenv.2011.04.038.
[12] J. Bayo, S. Olmos, J. López-Castellanos, Microplastics in an urban wastewater treatment plant: The influence of physicochemical parameters and environmental factors, Chemosphere 238 (2020) 12459, https://doi.org/10.1016/j.chemosphere.2019.124593.
[13] V.C. Shruti, F. Pérez-Guevara, I. Elizalde-Martínez, G. Kutralam-Muniasamy, First study of its kind on the microplastic contamination of soft drinks, cold tea and energy drinks - Future research and environmental considerations, Sci. Total Environ. 726 (2020) 138580, https://doi.org/10.1016/j.scitotenv.2020.138580.
[14] H. Bouwmeester, P.C. Hollman, R.J. Peters, Potential health impact of environmentally released micro-and nanoplastics in the human food production chain: experiences from nanotoxicology, Environ. Sci. Technol. 49 (15) (2015) 8932–8947, https://doi.org/10.1021/acs.est.5b01090.
[15] S. Xu, J. Ma, R. Ji, K.e. Pan, A.-J. Miao, Pan, Ai-Jun Miao, 2020, Microplastics in aquatic environments: Occurrence, accumulation, and biological effects, Sci. Total Environ. 703 (2020) 134699, https://doi.org/10.1016/j.scitotenv.2019.134699.
[16] C. Rivard, L. Moens, K. Roberts, J. Brigham, S. Kelley, Starch esters as biodegradable plastics: effects of ester group chain length and degree of substitution on anaerobic biodegradation, Enzyme Microbial Technol. 17 (9) (1995) 848–852, https://doi.org/10.1016/0141-0229(94)00120-G.
[17] D.K. Barnes, F. Galgani, R.C. Thompson, M. Barlaz, Accumulation and fragmentation of plastic debris in global environments, Philos. Trans. R. Soc. B 364 (2009) 1985–1998, https://doi.org/10.1098/rstb.2008.02.
[18] F. Corradini P. Meza R. Eguiluz F. Casado E. Huerta-Lwanga V. Geissen 671 2019 411 420.
[19] B. Henry, K. Laitala, I.G. Klepp, Microfibres from apparel and home textiles: Prospects for including microplastics in environmental sustainability assessment, Sci. Total Environ. 652 (2019) 483–494, https://doi.org/10.1016/j.scitotenv.2018.10.166.
[20] L. Su, S.M. Sharp, V.J. Pettigrove, N.J. Craig, B. Nan, F. Du, H. Shi, Superimposed microplastic pollution in a coastal metropolis, Water Res. 168 (2020) 115140, https://doi.org/10.1016/j.watres.2019.115140.
[21] H.P. Austin M.D. Allen B.S. Donohoe N.A. Rorrer F.L. Kearns R.L. Silveira B.C. Pollard G. Dominick R. Duman K. El Omari V. Mykhaylyk A. Wagner W.E. Michener A. Amore M.S. Skaf M.F. Crowley A.W. Thorne C.W. Johnson H.L. Woodcock J.E. McGeehan G.T. Beckham 115 19 2018 E4350 E4357.
[22] S.K. Kale A.G. Deshmukh M.S. Dudhare V.B. Patil Microbial degradation of plastic: a review J Biochem Tech 6 1 2015 pp. 952–961 ISSN: 0974–2328.
[23] Pathak, V.M. and Navneet, Review on the current status of polymer degradation: a microbial approach, Bioresour. Bioprocess. (2017) 4:15, DOI 10.1186/s40643-017-0145-9.
[24] C. Nerin, P. Alfaro, M. Aznar, C. Domeno, The challenge of identifying non-intentionally added substances from food packaging materials: A review, Anal. Chim. Acta 775 (2013) 14–24, https://doi.org/10.1016/j.aca.2013.02.028.

[25] J. Peng, J. Wang, L. Cai, Current understanding of microplastics in the environment: occurrence, fate, risks, and what we should do, Integr. Environ. Assess. Manag. 13 (3) (2017) 476–482, https://doi.org/10.1002/ieam.1912.
[26] M. Dong Q. Zhang X. Xing W. Chen Z. She Z. Luo 739 2020 139990 10.1016/j.scitotenv.2020.139990.
[27] L. Lv L. He S. Jiang J. Chen C. Zhou J. Qu Y. Lu P. Hong S. Sun C. Li 728 2020 138449 10.1016/j.scitotenv.2020.138449.
[28] P.R. Gogate, A.L. Prajapat, Depolymerization using sonochemical reactors: A critical review, Ultrason. Sonochem. 27 (2015) 480–494, https://doi.org/10.1016/j.ultsonch.2015.06.019.
[29] A. Fridman, Plasma Chemistry, Cambridge University Press, 2008.
[30] D. Dong, S. Tasaka, N. Inagaki, Thermal degradation of monodisperse polystyrene in bean oil, Polym Degrad Stab 72 (2) (2001) 345–351, https://doi.org/10.1016/S0141-3910(01)00031-3.
[31] A. Tayal, S.A. Khan, Degradation of a water-soluble polymer: molecular weight changes and chain scission characteristics, Macromolecules 33 (2000) 9488–9493, https://doi.org/10.1021/ma000736g.
[32] W.-M. Kulicke, A.H. Kull, W. Kull, H. Thielking, J. Engelhardt, J.-B. Pannek, Characterization of aqueous carboxymethylcellulose solutions in terms of their molecular structure and its influence on rheological behaviour, Polymer 37 (1996) 2723–2731, https://doi.org/10.1016/0032-3861(96)87634-8.
[33] T.h. Poinot, K. Benyahia, A. Govin, T.h. Jeanmaire, P.h. Grosseau, Use of ultrasonic degradation to study the molecular weight influence of polymeric admixtures for mortars, Constr. Build. Mater. 47 (2013) 1046–1052, https://doi.org/10.1016/j.conbuildmat.2013.06.007.
[34] N. Schittenhelm, W.-M. Kulicke, Producing homologous series of molar masses for establishing structure-property relationships with the aid of ultrasonic degradation, Macromol Chem Phys 201 (2000) 1976–1984, https://doi.org/10.1002/1521-3935(20001001)201:15<1976::AID-MACP1976>3.0.CO;2-0.
[35] K.N. Fotopoulou, H.K. Karapanagioti, Degradation of Various Plastics in the Environment, in: H. Takada, H.K. Karapanagioti (Eds.), Hazardous Chemicals Associated with Plastics in the Marine Environment, Hdb Env Chem, Springer International Publishing AG, 2017.
[36] B. Ranby, Photodegradation and photo-oxidation of synthetic polymers, J Anal Appl Pyrolysis 15 (1989) 237–247, https://doi.org/10.1016/0165-2370(89)85037-5.
[37] B. Singh, N. Sharma, Mechanistic implications of plastic degradation, Polym Degrad Stab 93 (3) (2008) 561–584, https://doi.org/10.1016/j.polymdegradstab.2007.11.008.
[38] I. Carpentieri, V. Brunella, P. Bracco, M.C. Paganini, E.M. Brach del Prever, M. P. Luda, S. Bonomi, L. Costa, Post irradiation oxidation of different polyethylenes, Polym Degrad Stab 96 (4) (2011) 624–629, https://doi.org/10.1016/j.polymdegradstab.2010.12.014.
[39] T. Zhao, P. Li, C. Tai, J. She, Y. Yin, Y. Qi, G. Zhang, Efficient decolorization of typical azo dyes using low-frequency ultrasound in presence of carbonate and hydrogen peroxide, J. Hazard. Mater. 346 (2018) 42–51, https://doi.org/10.1016/j.jhazmat.2017.12.009.
[40] J. Wang, Z. Wang, C.L.Z. Vieira, J.M. Wolfson, G. Pingtian, S. Huang, Review on the treatment of organic pollutants in water by ultrasonic technology, Ultrason. Sonochem. 55 (2019) 273–278, https://doi.org/10.1016/j.ultsonch.2019.01.017.
[41] M. Stucchi, C.L. Bianchi, C. Argirusis, V. Pifferi, B. Neppolian, G. Cerrato, D. C. Boffito, Ultrasound assisted synthesis of Ag-decorated TiO2 active in visible light, Ultrason. Sonochem. 40 (Pt A) (2018) 282–288, https://doi.org/10.1016/j.ultsonch.2017.07.016.
[42] D.J. Flannigan, K.S. Suslick, Plasma formation and temperature measurement during single-bubble cavitation, Nature 434 (7029) (2005) 52–55.
[43] T. Mason, J.P. Lorimer, Applied Sonochemistry: Uses of Power Ultrasound in Chemistry and Processing, Wiley-VCH, 2002.
[44] K.S. Suslick, D.A. Hammerton, R.E. Cline, Sonochemical hot spot, J Am Chem Soc. 108 (18) (1986) 5641–5642, https://doi.org/10.1021/ja00278a055.
[45] K.S. Suslick, Sonochemistry, Science 247 (4949) (1990) 1439–1445, https://doi.org/10.1126/science.247.4949.1439.
[46] M. Stucchi, C.L. Bianchi, C. Pirola, G. Cerrato, S. Morandi, C. Argirusis, G. Sourkouni, A. Naldoni, V. Capucci, Copper NPs decorated titania: A novel synthesis by high energy US with a study of the photocatalytic activity under visible light, Ultrason. Sonochem. 31 (2016) 295–301, https://doi.org/10.1016/j.ultsonch.2016.01.015.
[47] C. Vaitsis, G. Sourkouni, C. Argirusis, Metal Organic Frameworks (MOFs) and ultrasound: A review, Ultrason. Sonochem. 52 (2019) 106–119, https://doi.org/10.1016/j.ultsonch.2018.11.004.
[48] I. Tzanakis, D.G. Eskin, A. Georgoulas, D. Fytanidis, Incubation pit analysis and calculation.
[49] Bartis, et al., Eur. Phys. J. D 70 (2016) 25.
[50] T. Desmet, R. Morent, N. De Geyter, C. Leys, E. Schacht, P. Dubruel, Biomacromolecules 10 (2009) 2351.
[51] G. Da Ponte, E. Sardella, F. Fanelli, R. d'Agostino, P. Favia, Eur. Phys. J. Appl. Phys. 56 (2011) 24023.
[52] K. Fricke, S. Reuter, D. Schroeder, V. Schulz-von der Gathen, K.-D. Weltmann, T. von Woedtke, IEEE Trans. Plasma Sci. 40 (2012) 2900.
[53] A. Fridman (Ed.), Plasma Chemistry, Cambridge University Press, Cambridge, 2008.
[54] M.J. Pavlovich, H.-W. Chang, Y. Sakiyama, D.S. Clark, D.B. Graves, J. Phys. D 46 (2013), 145202.
[55] C.A.J. van Gils, S. Hofmann, B.K.H.L. Boekema, R. Brandenburg, P.J. Bruggeman, J. Phys. D 46 (2013), 175203.
[56] A. Starikovskiy, Y. Yang, Y.I. Cho, A. Fridman, Plasma Sources Sci. Technol. 20 (2011), 024003.
[57] P. Bruggeman, C. Leys, J. Phys. D 42 (2009), 053001.
[58] Y. Sakiyama D.B. Graves H.-W. Chang T. Shimizu G.E. Morfill 45 42 2012 425201 10.1088/0022-3727/45/42/425201.
[59] U. Kogelschatz, B. Eliasson, M. Hirth, Ozone Generation from Oxygen and Air: Discharge Physics and Reaction Mechanisms, Ozone Sci. Eng. 10 (4) (1988) 367–377, https://doi.org/10.1080/01919518808552391.
[60] P.R. Gogate, I.Z. Shirgaonkar, M. Sivakumar, P. Senthilkumar, N.P. Vichare, A. B. Pandit, Cavitation reactors: efficiency assessment using a model reaction, AIChE J. 47 (11) (2001) 2526–2538, https://doi.org/10.1002/(ISSN)1547-590510.1002/aic.v47:1110.1002/aic.690471115.
[61] S. Pasupuleti, G. Madras, Ultrasonic degradation of poly (styrene- co -alkyl methacrylate) copolymers, Ultrason. Sonochem. 17 (5) (2010) 819–826, https://doi.org/10.1016/j.ultsonch.2010.02.003.
[62] J.P. Lorimer, T.J. Mason, T.C. Cuthbert, E.A. Brookfield, Effect of ultrasound on the degradation of aqueous native dextran, Ultrason. Sonochem. 2 (1) (1995) S55–S57, https://doi.org/10.1016/1350-4177(94)00013-I.
[63] G.J. Price, P.F. Smith, Ultrasonic degradation of polymer solutions: 2. The effect of temperature, ultrasound intensity and dissolved gases on polystyrene in toluene, Polymer 34 (19) (1993) 4111–4117, https://doi.org/10.1016/0032-3861(93)90675-Z.
[64] D.R. Baer, S. Thevuthasan, in: Handbook of Deposition Technologies for Films and Coatings, Elsevier, 2010, pp. 749–864, https://doi.org/10.1016/B978-0-8155-2031-3.00016-8.
[65] M.H. Engelhard, T.C. Droubay, Y. Du, in: Encyclopedia of Spectroscopy and Spectrometry, Elsevier, 2017, pp. 716–724, https://doi.org/10.1016/B978-0-12-409547-2.12102-X.
[66] S. Krischok, O. Höfft, J. Günster, J. Stultz, D. Goodman, V. Kempter, H2O interaction with bare and Li-precovered TiO2: Studies with electron spectroscopies (MIES and UPS (HeI and II)), Surf. Sci. 495 (2001) 8–18.
[67] L. Klarhöfer, B. Roos, W. Viöl, O. Höfft, S. Dieckhoff, V. Kempter, W. Maus-Friedrichs, Valence band spectroscopy on lignin, Holzforschung (2008) 62, https://doi.org/10.1515/HF.2008.116.
[68] G. Binnig C.F. Quate C.h. Gerber 56 9 1986 930 933.
[69] F.J. Giessibl 75 3 2003 949 983.
[70] C.h. Roduit, S. Sekatski, G. Dietler, S. Catsicas, F. Lafont, S. Kasas, Stiffness Tomography by Atomic Force Microscopy, Biophys. J . 97 (2) (2009) 674–677, https://doi.org/10.1016/j.bpj.2009.05.010.
[71] N.J. Tao, S.M. Lindsay, S. Lees, Measuring the microelastic properties of biological material, Biophys. J . 63 (4) (1992) 1165–1169, https://doi.org/10.1016/S0006-3495(92)81692-2.
[72] G. Beamson, D. Briggs, High Resolution XPS of Organic Polymers: The Scienta ESCA300 Database, John Wiley & Sons Ltd (1992), https://doi.org/10.1002/pi.1994.210330424.
[73] N. De Geyter, R. Morent, T. Desmet, M. Trentesaux, L. Gengembre, P. Dubruel, C. Leys, E. Payen, Plasma modification of polylactic acid in a medium pressure DBD, Surf. Coat. Technol. 204 (20) (2010) 3272–3279, https://doi.org/10.1016/j.surfcoat.2010.03.037.
[74] E.M. Liston, L. Martinu, M.R. Wertheimer, Plasma surface modification of polymers for improved adhesion: a critical review, J. Adhesion Sci. Technol. 7 (10) (1993) 1091–1127.
[75] K. Yoshihisa, et al., Hydrophilic Modification of Plastic Surface by Using Microwave Plasma Irradiation, IHI Engineering Review 46 (1) (2013) 29.
[76] A.V. Tyurnina I. Tzanakis J. Morton J. Mi K. Porfyrakis B.M. Maciejewska N. Grobert D.G. Eskin Ultrasonic exfoliation of graphene in water: A key parameter study 168 2020 737 747.
[77] C.-M. Chan, T.-M. Ko, H. Hiraoka, Polymer surface modification by plasmas and photons, Surf. Sci. Rep. 24 (1-2) (1996) 1–54.
[78] F. Manenq S. Carlotti Mas, Some plasma treatment of PET fibres and adhesion testing to Rubber, A Angew. Makromol. Chem. Nr. 4698 271 (1999) 11 17.
[79] M. Morra, Occhiello,, E Contact Angle Hysteresis on Oxygen Plasma Treated Polypropylene Surfaces, J. colloid Interf. Sci. (1994) 95–111.
[80] X. Qi, Y. Ren, X. Wang, New advances in the biodegradation of poly(lactic) acid, Int. Biodeterior. Biodegrad. 117 (2017) 215–223.
[81] N. Omerović, M. Djisalov, K. Živojević, M. Mladenović, J. Vunduk, I. Milenković, N.Ž. Knežević, I. Gadjanski, J. Vidić, Antimicrobial nanoparticles and biodegradable polymer composites for active food packaging applications, Compr. Rev. Food Sci. Food Saf. 20 (3) (2021) 2428–2454.
[82] M. Ponjavic, M.S. Nikolic, J. Nikodinovic-Runic, S. Jeremic, S. Stevanovic, J. Djonlagic, Degradation behaviour of PCL/PEO/PCL and PCL/PEO block copolymers under controlled hydrolytic, enzymatic and composting conditions, Polym. Test. 57 (2017) 67–77.
[83] Nikolaivits E., et al., Progressing Plastics Circularity: A Review of Mechano-Biocatalytic Approaches for Waste Plastic (Re)valorization, Front. Bioeng. Biotechnol. | doi: 10.3389/fbioe.2021.696040.
[84] W. Pattanasuttichonlakul, N. Sombatsompop, B. Prapagdee, Accelerating biodegradation of PLA using microbial consortium from dairy wastewater sludge combined with PLA-degrading bacterium, Int. Biodeterior. Biodegrad. 132 (2018) 74–83.